Angewandte Chemie

GDCh

Eine Zeitschrift der Gesellschaft Deutscher Chemiker

www.angewandte.de

Akzeptierter Artikel

Titel: Unravelling the Complexities of Pseudocontact Shift Analysis in Lanthanide Coordination Complexes of Differing Symmetry

Autoren: David Parker, Elizaveta Suturina, Alice Harnden, Andrei Batsanov, Mark Fox, Kevin Mason, Michele Vonci, Eric McInnes, and nicholas chilton

Zitierweise: *Angew. Chem. Int. Ed.* 10.1002/anie.201906031
Angew. Chem. 10.1002/ange.201906031

Link zur VoR: http://dx.doi.org/10.1002/anie.201906031
http://dx.doi.org/10.1002/ange.201906031

WILEY-VCH

10.1002/ange.201906031

WILEY-VCH

Unravelling the Complexities of Pseudocontact Shift Analysis in Lanthanide Coordination Complexes of Differing Symmetry

Alice C. Harnden,[a] Elizaveta A. Suturina,[b] Andrei S. Batsanov,[a] Mark A. Fox,[a] Kevin Mason,[a] Michele Vonci,[c] Eric J. L. McInnes,[c] Nicholas F Chilton[c] and David Parker*[a]

Abstract: In two closely related series of eight-coordinate lanthanide complexes, a switch in the sign of the dominant ligand field parameter and striking variations in the sign, amplitude and orientation of the main component of the magnetic susceptibility tensor as the Ln^{3+} ion is permuted conspire to mask modest changes in NMR paramagnetic shifts, but are evident in Yb EPR and Eu emission spectra.

Lanthanide induced shift and paramagnetic relaxation enhancement are subjects of continuous research driven by new applications of lanthanide complexes as tags for biomolecular structure analysis,[1] and PARASHIFT probes for magnetic resonance imaging (MRI).[2] While Gd^{3+} tags are employed in double electron-electron resonance (DEER) distance measurements in biomolecules,[3] and Gd^{3+} MRI contrast agents are routinely used,[4] non-Gd tags with pronounced magnetic anisotropy continue to challenge existing theoretical models of paramagnetic shift[5] and relaxation.[6] Many of the conclusions made in the early literature examining NMR behaviour in paramagnetic lanthanide systems, for example, may have low significance because of the limitations of Bleaney's theory of magnetic anisotropy.[7] Often, unreasonable estimations of a contact contribution were invoked in order to allow experimental data to be fitted, and sometimes 'distance only' dependent relaxation rate data were used to aid assignment, notwithstanding the fact that the electron-nuclear dipolar interaction has been shown to have a strong directional dependence, both in the dipolar and the Curie contributions to paramagnetic relaxation.[6]

The theory of Bleaney assumed that ligand field (zero-field) splitting of the ground *J*-multiplet is less than *kT* and that the ligand-field parameters are invariant as the lanthanide ion is permuted in an isostructural series. Neither assumption is appropriate for most lanthanide complexes, and recent work has highlighted the exquisite sensitivity of the ligand field to minor structural perturbation,[8] exemplified by the dramatic changes in NMR pseudocontact shifts and Eu emission spectral form that occur following a change of solvent or in the degree of aggregation for systems with a small ligand field (<kT), where no solvent is metal-bound.[9] Indeed, such studies have emphasised the need for very careful magneto-structural correlations, so that the size, sign and orientation of the principal components of the magnetic susceptibility tensor can be reliably determined, as they vary for each different lanthanide complex of a common ligand.

Pseudocontact shifts (PCS) dominate the experimental ^{1}H NMR paramagnetic shifts in 4*f*-block coordination complexes, as the unpaired electron spin populations on ligand protons are generally very small.[5a, 9b] Such shifts can be described by the McConnell equation:[10]

$$\delta^{PCS} = \frac{1}{12\pi r^3}\left[\chi_{ax}\left(3\cos^2\theta - 1\right) + 3\chi_{rh}\sin^2\theta\cos 2\varphi\right] \qquad (1)$$

where r, θ and φ are nuclear polar coordinates, with respect to the lanthanide ion, in the eigenframe of the magnetic susceptibility tensor. The terms χ_{ax} and χ_{rh} represent the axiality and rhombicity of the tensor, wherein χ_{rh} has a limit of 1/3 of χ_{ax}.

Here, we examine the spectroscopic behavior of selected C_1- and C_2-symmetric lanthanide complexes [LnL^1] and [LnL^2]$^+$, which are model systems for the temperature and pH dependent PARASHIFT probes being developed in parallel.[2a, 2b] Previous work has shown that the magnetic susceptibility tensor can vary from nearly fully rhombic for Tm^{3+} to almost fully axial for Tb^{3+} and Dy^{3+} in [LnL^{1a}] with the sign of axiality being negative for Tb^{3+}-Ho^{3+} and positive for Er^{3+}-Yb^{3+}.[5a, 9b] The corresponding diamagnetic Y^{3+} complexes were used to examine in detail the static and dynamic aspects of complex stereoisomerism, and served as the starting point for computational studies and PCS analysis, aided by the X-ray structural determination of the neutral Yb^{3+} complex of L^{1b}, and the cationic Yb^{3+} complex of L^2.

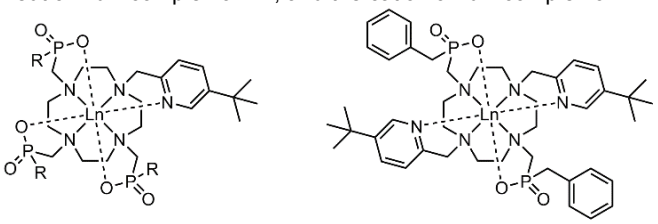

[LnL^1] a) R = Me
b) R = CH_2Ph

[LnL^2]$^+$

Scheme 1. Molecular structures of the complexes examined in this study.

The lanthanide complexes of L^{1b} and L^2 were prepared in a similar manner to the corresponding series based on the P-Me triphosphinate ligand, L^{1a},[11] and were purified by reverse-phase HPLC, or crystallized by diffusion of Et_2O into a methanol solution (see SI). The cationic complexes, [LnL^2]$^+$, were isolated as their hexafluorophosphate salts. X-ray crystal structures at 120 K revealed the Ln(III) ions adopting a twisted square anti-prismatic (TSAP) eight-coordinate geometry with no bound solvent. All complexes crystallized in centrosymmetric space groups, viz. $P2_1/c$ for [YbL^{1b}]·3.5MeOH, $P\bar{1}$ for both [YbL^2][PF_6]

[a] Dr A. C. Harnden, Dr A. S. Batsanov, Dr M. A. Fox, Dr K. Mason, Prof D. Parker
Department of Chemistry
Durham University
South Road, Durham, DH1 3LE, United Kingdom
david.parker@durham.ac.uk
[b] Dr E. A. Suturina
Department of Chemistry
University of Bath
Claverton Down, Bath BA2 7AY, United Kingdom
[c] Dr M. Vonci, Prof E. J. McInnes, Dr N. F. Chilton
School of Chemistry and Photon Science Institute,
The University of Manchester
Oxford Road, Manchester, M13 9PL, United Kingdom

Supporting information for this article is given via a link at the end of the document.

10.1002/ange.201906031

·3MeOH and (non-isomorphous) $[TbL^2][PF_6]$·6MeOH. Thus, in each crystal structure both enantiomers were present equally, with the configurations (RRR)-Λ-(λλλλ) or (SSS)-Δ-(δδδδ) for $[YbL^{1b}]$, (RR)-Λ–(λλλλ) or (SS)-Δ-(δδδδ) for $[LnL^2][PF_6]$ defining the chirality at phosphorus, the ring helicity and the twist of the NCCN chelate rings respectively (Figure 1). Both phosphinate oxygen atoms in $[YbL^2]^+$ and two out of three in $[YbL^{1b}]$ accepted hydrogen bonds from methanol molecules of crystallization. The average distances between the lanthanide ion and the hydrogen atoms of the ^{t}Bu NMR reporter group were similar and were found to be 6.74 Å in $[YbL^2]^+$ and 6.62 Å in $[YbL^{1b}]$. In the twisted square antiprismatic geometry (TSAP), the degree of 'twist' between the macrocyclic N_4 plane and the N_2O_2 or NO_3 planes was 26.4° for $[YbL^{1b}]$, near identical to that found for $[YbL^{1a}]$.[11] However, with $[YbL^2]^+$ this twist angle was reduced to 18.5°, reflecting the impact of the additional pyridine chelate ring moiety on the degree of twist, (Tables S1-4).

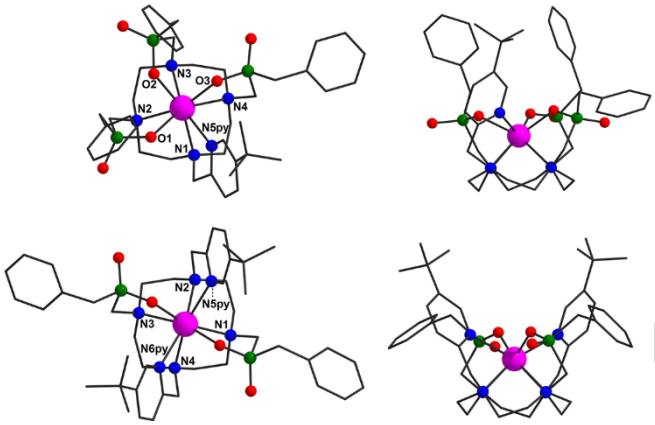

Figure 1. (*upper*) Molecular structure of (SSS) - Δ - (δδδδ) $[Yb.L^{1b}]$ viewed from the top and side; H atoms are omitted for clarity; (*lower*) views of the structure of (RR) -Λ – (λλλλ) – $[Yb.L^2]$; CCDC: 1896115-116.

Density functional theory (DFT) geometry optimizations were undertaken for Y(III) analogues where many possible conformers within the various stereoisomers were analysed. At the M06-2X/6-31G(d)/Stuttgart-ECP SMD-methanol model chemistry,[11] the TSAP (RRR)-Λ–(λλλλ) stereoisomer for $[YL^{1b}]$ was lowest in energy by ca 6.4 kJ mol^{-1} and the TSAP (RR)-Λ–(λλλλ) stereoisomer for $[YL^2]^+$ by about 6.3 kJ mol^{-1} (Figure S1, Tables S5 and S6). These lowest energy conformers are also observed in X-ray structures of $[YbL^{1b}]$ and $[YbL^2]^+$.

A full NMR assignment of the ^{1}H, ^{13}C and ^{31}P resonances of $[YL^{1b}]$ and $[YL^2]^+$ in CD_3OD was achieved using a combination of two-dimensional ^{1}H-^{1}H NOESY, ^{1}H-^{1}H COSY, ^{1}H-^{13}C/^{31}P HMBC, ^{1}H-^{13}C HSQC and Pureshift NMR techniques (SI Figures S3 and Table S10, for example, for the assignment of the 43 protons and 34 carbons in $[YL^{1b}]$).[12] With $[YL^{1b}]$, two isomers were observed in a 10:1 ratio, (*cf.* 5:1 in $[YL^{1a}]$[11]), most clearly defined in the ^{31}P NMR spectrum where each phosphorus nucleus resonated as an ^{89}Y coupled doublet, (^2J = 6 Hz). For $[YL^2]^+$, only one phosphorus resonance was observed for the major stereoisomer (70%), consistent with the presence of time-averaged C_2 symmetry in solution. In each case, the major species revealed the presence of only one strong NOE signal between the exocyclic pyridyl CH_2 and the macrocycle CH_2 resonances. The occurrence of this singular NOE correlation, between the axial proton on the C_2 carbon of the cyclen 12-N_4 ring and the 'axial' exocyclic CH_2 pyridyl proton has been shown to be consistent only with a TSAP coordination geometry.[11, 13]

Furthermore, the two possible TSAP isomers (RRR)/(RR)-Λ–(λλλλ) and (RRR)/(RR)-Δ–(δδδδ) can be distinguished by NOE spectroscopy. Inspection of the optimized structures of each TSAP isomer showed that the ^{1}H-^{1}H distance between the benzylic CH_2 and ring 'cyclen' protons should be about 2.1 Å (strong NOE) in (RRR)/(RR)-Δ–(δδδδ) whereas this distance is ca 2.6 Å in the (RRR)/(RR) –Λ –(λλλλ) diastereoisomer. No NOE was observed between these resonances, supporting the presence of TSAP (RRR)/(RR) –Λ –(λλλλ) diastereoisomers in solution. Observation of a relatively weak NOE between the benzylic PCH_2 resonances and the proximate ^{t}Bu and pyH_6 protons confirmed the solution assignment in each case, consistent with the X-ray structural analyses. The rate of exchange between the minor and major isomer of $[YL^{1b}]$ was found to be 1.27 s^{-1}. The reverse rate was slower (0.12 s^{-1}), and the equilibrium constant calculated from these rates (K_{eq} = 10.9) was found to be in good agreement with that calculated by integration of the fully relaxed ^{31}P NMR spectrum (10:1). The forward and reverse rates of the exchange of the isomers were broadly similar in the case of $[YL^2]$Cl (k = 0.87 – 1.28 s^{-1}, k^{-1} = 0.14 – 0.18 s^{-1}). Indeed, rates of these exchange processes are similar to those found for both $[YL^{1b}]$ and $[YL^{1a}]$.

In the interest of using these compounds as model systems for PARASHIFT probes, the ^{1}H NMR chemical shift of the *tert*-butyl reporter group for selected lanthanide complexes (Tb-Yb) was measured (Figure 2). A simple interpretation of these shifts would suggest that similar magnetic anisotropies exist, with only a slight reduction in the magnitude in the $[LnL^2]^+$ series.

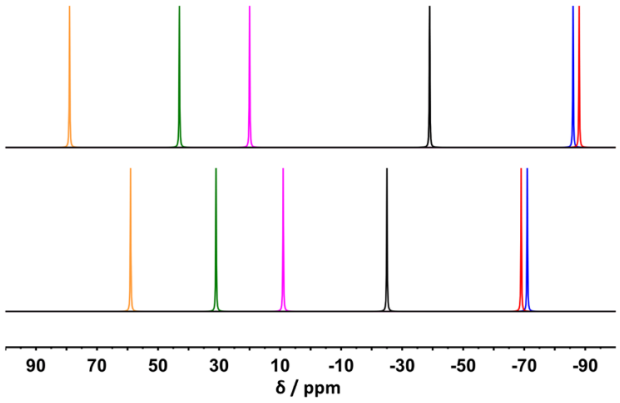

Figure 2. Schematic representation of the experimentally measured chemical shifts of the major *tert*-butyl signals in $[LnL^{1b}]$ (*top*) and $[LnL^2]$Cl (*bottom*) (CD_3OD, 11.7 T, 295 K) (yellow - Tm, green - Er, magenta - Yb, black – Ho, red - Dy, blue - Tb).

To delve further into the cause of these shifts, proton and ^{31}P NMR analyses of the Yb^{3+} complexes of L^{1b} and L^2 were undertaken over a range of magnetic fields (1 to 16.5T). For $[Yb.L^{1b}]$, two isomers were observed (12:1) and with $[YbL^2]^+$ three species could be discerned in ratio 10:2:0.5, with the major species possessing time-averaged C_2-symmetry, (Figures S11-S14). Using a semi-automated combinational assignment procedure in Spinach,[14] the PCS data were assigned for every ^{1}H resonance of the major species, (except the benzyl resonances), aided by the prior Y^{3+} complex assignments.

Both DFT optimized and XRD structures of $[YbL^{1b}]$ and $[YbL^2]^+$ have been used in the pNMR analysis (Tables S12 and S13). By fitting equation (1) to the traceless part of the magnetic susceptibility tensor, the high quality of the fits (R^2 > 0.997 in each case with DFT structures, see SI: Figure S15, Table S13)

10.1002/ange.201906031

allowed the corresponding pseudocontact shift fields to be constructed (Figure 3). The 'best-fit' susceptibility tensors are described by their axiality and rhombicity parameters, together with the three Euler angles, with respect to the molecular frame, (Table 1). Comparing data for [YbL^{1a}] and [YbL^{1b}], the structural modification from methyl to benzylphosphinate groups has a rather small impact on the amplitude, shape and orientation of the PCS fields. However, comparing PCS fields for [YbL^{1b}] and [YbL^{2}]$^{+}$, dramatic changes in the PCS fields were found, (Figure 3). The magnetic anisotropy has changed sign, but the negative PCS lobe is still oriented in the "equatorial plane" of the molecule, because of a 90° switch in the orientation of the main magnetic axis. Such behaviour is consistent with a change in the sign of the second order ligand field parameter B_0^2.

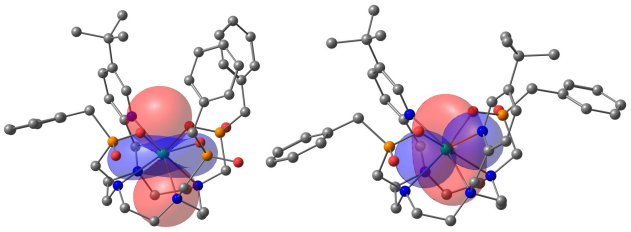

Figure 3. Pseudocontact shift fields, reconstructed using the 'best fit' susceptibility tensor for [YbL^{1b}] (left) and [YbL^{2}]$^{+}$ (right); positive PCS is shown in red (+200 ppm), negative in blue (-200 ppm) (see Table 1).

Table 1. Magnetic susceptibility tensors (SI units) of [YbL^{1a}], [YbL^{1b}] and [YbL^{2}]$^{+}$, obtained by fitting paramagnetic NMR chemical shift data (4.7 T, CD_3OD, 295 K) and computed with SINGLE_ANISO[15] using the DFT optimized structures (in parentheses), expressed in terms of axiality (χ_{ax}), rhombicity (χ_{rh}) and Euler angles. See SI for the convention used.

Complex	χ_{ax} ($Å^3$)	χ_{rh}/χ_{ax}	α(°)	β(°)	γ(°)
[YbL^{1a}]	0.11 (0.14)	0.13 (0.11)	185 (204)	23 (30)	211 (21)
[YbL^{1b}]	+0.13 (0.16)	0.11 (0.08)	168 (239)	22 (25)	171 (345)
[YbL^{2}]$^{+}$	-0.09 (-0.09)	0.10 (0.14)	70 (241)	90 (89)	269 (84)

Information on the sign and size of B_0^2 is readily accessible by analysis of the emission spectrum of the corresponding Eu^{3+} complexes in methanol, Figure 4. [16] The values of B_0^2 and B_2^2 for [EuL^{2}]$^{+}$ were found to be +923 and -153 cm^{-1}, contrasting with values of -703 and -167 cm^{-1} for [EuL^{1b}] and -596 and -228 cm^{-1} for [EuL^{1a}]. In water, the corresponding values were: [EuL^{2}]$^{+}$, B_0^2. = +735 cm^{-1}, B_2^2= -220 cm^{-1}; [EuL^{1b}], B_0^2. = -650 cm^{-1}, B_2^2 =- 80 cm^{-1} and -660 and -122 cm^{-1} for [EuL^{1a}],[5a]; ligand field parameters are given here in the spherical tensor formalism.

The confirmation of the change in sign of B_0^2 for the complexes of L^{1a} and L^{2} is supportive of the hypothesis that for these three complexes, the cooperative effect of the change in size and orientation of the major component of the magnetic susceptibility tensor and the inversion of the sign of the ligand field conspire to mask the complexity of changes in pseudocontact shift behaviour.

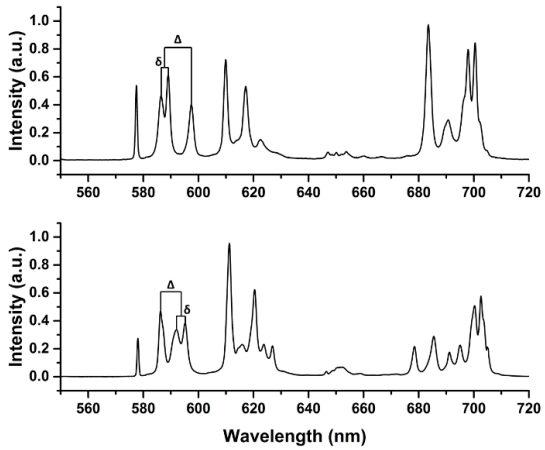

Figure 4. Emission spectra (295K, CH_3OH, λ_{ex} 270mm) of [EuL^{2}]$^{+}$ (*upper*) and [Eu.L^{1b}] (*lower*) highlighting splitting of the Δ *J*= 1 manifold, where $\Delta = 3B_0^2$ and $\delta = -2\sqrt{6}\,B_2^2$ in the spherical operator formalism.

Changes in the sign of B_0^2 in closely related structures have been observed relatively rarely,[17] e.g. in systems that switch from a TSAP to a SAP coordination geometry, where the twist angle changes by about +10°. Here, the change in angle is around -8° for [YbL^{1b}] *vs* [YbL^{2}]. The sensitivity of lanthanide ligand fields to distortion has been noted in theoretical work.[18]

When the position of the principal magnetic axis changes orientation, the ordering of the M_J sub-levels in a lanthanide complex will alter as well. Such a change is most readily observed by examining very low temperature EPR spectra, from which information on the magnetic anisotropy of the ground state can be ascertained.[5b-e] X-band continuous wave EPR spectra were collected at 5 K for solid crystalline and frozen solution (95% MeOH + 5% Et_2O) samples of [YbL^{2}] and [YbL^{1b}]. The 5 K spectra can be simulated with the effective *S* = ½ model, which is appropriate for the Kramers $^2F_{7/2}$ Yb^{3+} ion where only the lowest energy doublet is populated at 5 K, along with hyperfine coupling to the ^{171}Yb and ^{173}Yb nuclei (*I* = 1/2 and 5/2, respectively, with natural abundances of 14.2% and 16.1%). Simulations, using Easyspin,[19] give "easy-axis-like" (5.25, 2.63, 2.08) and "easy-plane-like" (4.22, 3.60, 2.38) effective *g*-tensors for [YbL^{1b}] and [YbL^{2}], respectively (Figures 5 and S16; Tables S16 and S17). The pairs of spectra in the solid state and solution phases are very similar, with only very minor changes in g_{eff}, strongly suggesting that no solvent coordination occurs. *Ab initio* CASSCF-SO calculations using both the XRD structures (including the two crystallographically independent molecules of [YbL^{1b}]) and the DFT-optimized structures (see SI) have been performed to elucidate the electronic structure and magnetic anisotropy of the Yb^{3+} complexes. The CASSCF-SO calculated effective *g*-values for the ground Kramers doublets (Table S16) agree very well with those obtained by EPR, confirming the same "easy-axis-like" *vs* "easy-plane-like" anisotropies. The calculations show that the main magnetic axis that corresponds to the smallest g-value in [YbL^{2}] has a large tilt angle of β=74 degrees (Figure 5). In [YbL^{1b}] the orientation of the largest effective *g*-value is tilted only by β = 35 degrees (Figure 5). These results correlate with the differences in the orientation of the high temperature magnetic susceptibility tensor (angle β in Table 1) and the differences in luminescence spectra (Figure 4).

10.1002/ange.201906031

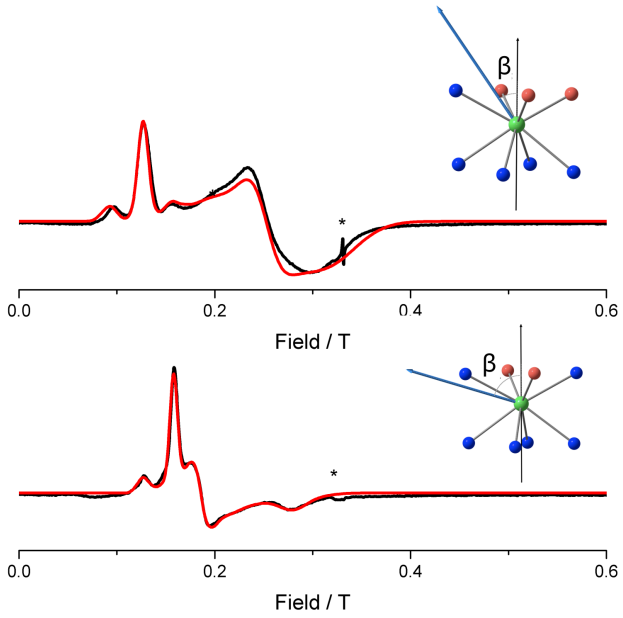

Figure 5 CW X-band EPR spectra of [YbL^{1b}] (*upper*) and [YbL^{2}] (*lower*) as a frozen solution (95% MeOH, 5% Et_2O) at 5K. Experimental spectra are in black and simulations are in red, each inset shows the orientation of the main magnetic axis calculated by CASSCF-SO, based on the DFT optimized structures (Yb – green, N – blue, O - red). Calculated and measured g-values are in Table S15, simulation parameters in Table S16. Signals marked with an asterisk (*) are spurious weak signals in the resonator and not intrinsic to the sample.

In conclusion, it has always been assumed – partly as a consequence of dogged adherence to Bleaney theory – that the sign of the ligand field parameter B_0^2 governs the sense of observed NMR pseudocontact shifts and its size determines their magnitude. Here, we show for the first time that this hypothesis may not hold. The crystal field splitting and the size, sign and orientation of the major component of the magnetic susceptibility tensor need to be considered when interpreting experimental pseudo-contact shift data. Here, B_0^2 is positive for Ln^{3+} complexes of L^2 while it is negative and of smaller magnitude for complexes of L^{1b}, and yet, counter-intuitively, the pseudocontact shifts are both in the same direction and are largest for complexes of L^{1b}. Evidently, this study suggests a need to exercise caution in the use of PCS data for structural analyses, and indicates the need to understand better the link between the ordering of the M_J sub-levels for a given Ln^{3+} ion, their relative Boltzmann population and the overall magnetic susceptibility size and anisotropy at a given temperature. Such an understanding has parallels in the quest for high-temperature, single molecule magnets, where the order and energy separation of the various M_J levels is of paramount importance.

Acknowledgements

We thank EPSRC for support (EP/N006909/1; L01212X; N006895/1) including funding of the National EPR Facility, Bath University for a Fellowship, and Dr. D.S. Yufit for assistance with X-ray structural determinations. This paper is dedicated to the one who is always there.

Keywords: lanthanide • coordination • EPR • NMR • emission

References

[1] a) T. Müntener, J. Kottelat, A. Huber, D. Häussinger, *Bioconjugate Chem.* **2018**, *29*, 3344-3351; b) C. Nitsche, G. Otting, *Prog. Nucl. Magn. Reson. Spectrosc.* **2017**, *98-99*, 20-49; c) B.-B. Pan, F. Yang, Y. Ye, Q. Wu, C. Li, T. Huber, X.-C. Su, *Chem. Commun.* **2016**, *52*, 10237-10240; d) E. A. Suturina, I. Kuprov, *Phys. Chem. Chem. Phys.* **2016**, *18*, 26412-26422; e) M. D. Lee, M. L. Dennis, J. D. Swarbrick, B. Graham, *Chem. Commun.* **2016**, *52*, 7954-7957; f) E. Ravera, G. Parigi, C. Luchinat, *J. Magn. Reson.* **2017**, *282*, 154-169.

[2] a) K.-L. N. A. Finney, A. C. Harnden, N. J. Rogers, P. K. Senanayake, A. M. Blamire, D. O'Hogain, D. Parker, *Chem.: Eur. J.* **2017**, *23*, 7976-7989; b) P. K. Senanayake, N. J. Rogers, K.-L. N. A. Finney, P. Harvey, A. M. Funk, J. I. Wilson, D. O'Hogain, R. Maxwell, D. Parker, A. M. Blamire, *Magn. Reson. Med.* **2017**, *77*, 1307-1317; c) A. C. Harnden, D. Parker, N. J. Rogers, *Coord. Chem. Rev.* **2019**, *383*, 30-42.

[3] a) D. Goldfarb, *Phys. Chem. Chem. Phys.* **2014**, *16*, 9685-9699; b) G. Prokopiou, M. D. Lee, A. Collauto, E. H. Abdelkader, T. Bahrenberg, A. Feintuch, M. Ramirez-Cohen, J. Clayton, J. D. Swarbrick, B. Graham, G. Otting, D. Goldfarb, *Inorg. Chem.* **2018**, *57*, 5048-5059; c) A. Shah, A. Roux, M. Starck, J. A. Mosely, M. Stevens, D. G. Norman, R. I. Hunter, H. El Mkami, G. M. Smith, D. Parker, J. E. Lovett, *Inorg. Chem.* **2019**, *58*, 3015-3025; d) E. A. Suturina, D. Häussinger, K. Zimmermann, L. Garbuio, M. Yulikov, G. Jeschke, I. Kuprov, *Chem. Sci.* **2017**, *8*, 2751-2757.

[4] P. Caravan, J. J. Ellison, T. J. McMurry, R. B. Lauffer, *Chem. Rev.* **1999**, *99*, 2293-2352.

[5] a) E. A. Suturina, K. Mason, C. F. G. C. Geraldes, I. Kuprov, D. Parker, *Angew. Chem. Int. Ed.* **2017**, *56*, 12215-12218; b) O. A. Blackburn, R. M. Edkins, S. Faulkner, A. M. Kenwright, D. Parker, N. J. Rogers, S. Shuvaev, *Dalton Trans.* **2016**, *45*, 6782-6800; c) G. Castro, M. Regueiro-Figueroa, D. Esteban-Gómez, P. Pérez-Lourido, C. Platas-Iglesias, L. Valencia, *Inorg. Chem.* **2016**, *55*, 3490-3497; d) E. Kreidt, C. Bischof, C. Platas-Iglesias, M. Seitz, *Inorg. Chem.* **2016**, *55*, 5549-5557; e) D. Esteban-Gómez, L. A. Büldt, P. Pérez-Lourido, L. Valencia, M. Seitz, C. Platas-Iglesias, *Inorg. Chem.* **2019**, *58*, 3732-3743; f) G. Parigi, L. Benda, E. Ravera, M. Romanelli, C. Luchinat, *J. Chem. Phys.* **2019**, *150*, 144101; g) L. Benda, J. Mareš, E. Ravera, G. Parigi, C. Luchinat, M. Kaupp, J. Vaara, *Angew. Chem. Int. Ed.* **2016**, *55*, 14713-14717.

[6] a) E. A. Suturina, K. Mason, C. F. G. C. Geraldes, N. F. Chilton, D. Parker, I. Kuprov, *Phys. Chem. Chem. Phys.* **2018**, *20*, 17676-17686; b) N. J. Rogers, K.-L. N. A. Finney, P. K. Senanayake, D. Parker, *Phys. Chem. Chem. Phys.* **2016**, *18*, 4370-4375.

[7] B. Bleaney, *J. Magn. Reson. (1969)* **1972**, *8*, 91-100.

[8] a) M. Vonci, K. Mason, E. A. Suturina, A. T. Frawley, S. G. Worswick, I. Kuprov, D. Parker, E. J. L. McInnes, N. F. Chilton, *J. Am. Chem. Soc.* **2017**, *139*, 14166-14172; b) M. Vonci, K. Mason, E. R. Neil, D. S. Yufit, E. J. L. McInnes, D. Parker, N. F. Chilton, *Inorg. Chem.* **2019**.

[9] a) A. W. J. Poh, J. A. Aguilar, A. M. Kenwright, K. Mason, D. Parker, *Chem.: Eur. J.* **2018**, *24*, 16170-16175; b) K. Mason, A. C. Harnden, C. W. Patrick, A. W. J. Poh, A. S. Batsanov, E. A. Suturina, M. Vonci, E. J. L. McInnes, N. F. Chilton, D. Parker, *Chem. Commun.* **2018**, *54*, 8486-8489.

[10] H. M. McConnell, *J. Chem. Phys.* **1957**, *27*, 226-229.

[11] K. Mason, N. J. Rogers, E. A. Suturina, I. Kuprov, J. A. Aguilar, A. S. Batsanov, D. S. Yufit, D. Parker, *Inorg. Chem.* **2017**, *56*, 4028-4038.

[12] a) M. Foroozandeh, R. W. Adams, N. J. Meharry, D. Jeannerat, M. Nilsson, G. A. Morris, *Angew. Chem. Int. Ed.* **2014**, *53*, 6990-6992; b) J. A. Aguilar, J. Cassani, M. Delbianco, R. W. Adams, M. Nilsson, G. A. Morris, *Chem.: Eur. J.* **2015**, *21*, 6623-6630.

[13] L. D. Bari, G. Pintacuda, P. Salvadori, R. S. Dickins, D. Parker, *J. Am. Chem. Soc.* **2000**, *122*, 9257-9264.

[14] H. J. Hogben, M. Krzystyniak, G. T. P. Charnock, P. J. Hore, I. Kuprov, *J. Magn. Reson.* **2011**, *208*, 179-194.

[15] L. Ungur, L. F. Chibotaru, *Chem.: Eur. J.* **2017**, *23*, 3708-3718.

[16] a) C. Görller-Walrand, K. Binnemans, in *Handbook on the Physics and Chemistry of Rare Earths, Vol. 23*, Elsevier, **1996**, pp. 121-283; b) K. Binnemans, C. Görller-Walrand, *Chem. Phys. Lett.* **1995**, *245*, 75-78.

[17] a) M. P. Lowe, D. Parker, O. Reany, S. Aime, M. Botta, G. Castellano, E. Gianolio, R. Pagliarin, *J. Am. Chem. Soc.* **2001**, *123*, 7601-7609; b) T. Krchová, V. Herynek, A. Gálisová, J. Blahut, P. Hermann, J. Kotek,

10.1002/ange.201906031

Inorg. Chem. **2017**, *56*, 2078-2091; c) S. Shuvaev, E. A. Suturina, K. Mason, D. Parker, *Chem. Sci.* **2018**, *9*, 2996-3003.
[18] V. S. Mironov, Y. G. Galyametdinov, A. Ceulemans, C. Görller-Walrand, K. Binnemans, *J. Chem. Phys.* **2002**, *116*, 4673-4685.
[19] S. Stoll, A. Schweiger, *J. Magn. Reson.* **2006**, *178*, 42-55.

10.1002/ange.201906031

WILEY-VCH

Entry for the Table of Contents

COMMUNICATION

In two closely related series of lanthanide complexes, a switch in the sign of the dominant ligand field parameter and striking variations in the sign, amplitude and orientation of the main component of the magnetic susceptibility tensor as the Ln^{3+} ion is permuted mask modest changes in NMR paramagnetic shifts, but are evident in Yb EPR and Eu emission spectra.

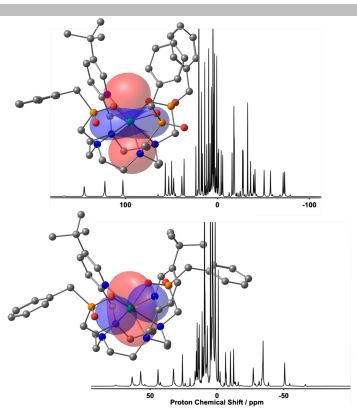

*Alice C. Harnden, Elizaveta A. Suturina, Andrei S. Batsanov, Mark A. Fox, Kevin Mason, Michele Vonci, Eric J. L. McInnes, Nicholas F Chilton and David Parker**

Page No. – Page No.

Unravelling the Complexities of Pseudocontact Shift Analysis in Lanthanide Coordination Complexes of Differing Symmetry